CJC Chinese Journal of Chemistry
中国化学 - An International Journal

Accepted Article

Title: Design, Synthesis and Biological Evaluation of Novel α-Acyloxycarboxamide-Based Derivatives as c-Met Inhibitors

Authors: Yu-juan Feng, Yu-Lin Ren,* Li-Ming Zhao,* Guo-Qiang Xue, Wen-Hao Yu, Jia-Qi Yang, and Jun-Wei Liu

This work may now be cited as: *Chin. J. Chem.* **2021**, *39,* 10.1002/cjoc.202100106.

The final Version of Record (VoR) of it with formal page numbers will soon be published online in Early View: http://dx.doi.org/10.1002/cjoc.202100106.

WILEY-VCH SIOC CCS

ISSN 1001-604X • CN 31-1547/O6
mc.manuscriptcentral.com/cjoc
www.cjc.wiley-vch.de

CJC ChineseJournal of Chemistry 中国化学 AnInternationalJournal

For submission:https://mc.manuscriptcentral.com/cjoc
For published articles:https://onlinelibrary.wiley.com/journal/16147065

Concise Report

Cite this paper: *Chin. J. Chem.* **2021**, *39*, XXX—XXX. **DOI: 10.1002/cjoc.202100XXX**

Design, Synthesis and Biological Evaluation of Novel α-Acyloxycarboxamide-Based Derivatives as c-Met Inhibitors

Yu-juan Feng,[‡,a,b] Yu-Lin Ren,[*,‡,a,b] Li-Ming Zhao,[*,a,b] Guo-Qiang Xue,[a,b] Wen-Hao Yu,[a,b] Jia-Qi Yang,[a,b] and Jun-Wei Liu [a,b]

[a] *Northwest Minzu University, Lanzhou, Gansu 730030, China*
[b] *Department of Public Health, The Second Provincial People's Hospital of Gansu, Lanzhou, Gansu 730030, China*

Keywords

4-(2-Fluorophenoxy)quinoline derivatives | c-Met inhibitors | Passerini reaction | α-Acyloxycarboxamide | Biological evaluation

Main observation and conclusion

Dysregulated HGF/c-Met signalling has been associated with many human cancers, poor clinical outcomes, and even resistance acquisition to some approved targeted therapies. As such, c-Met kinase has emerged as a attractive target for anticancer drug discovery. Herein, a series of 6,7-disubstitued-4-(2-fluorophenoxy)quinoline derivatives bearing α-acyloxycarboxamide moiety were designed, synthesized *via* Passerini reaction as the key step, and evaluated for their *in vitro* biological activities against c-Met kinase and five selected cancer cell lines. The preliminary structure-activity relationship demonstrated that α-acyloxycarboxamide as the 5-atom linker maintained the potent antitumor potency. Among these compounds, compound **25s** (c-Met IC_{50} = 4.06 nM) was identified as the most promising lead compound and displayed the most potent antiproliferative activities against A549, HT-29 and MDA-MB-231 cell lines with IC_{50} of 0.39, 0.20, and 0.58 μM, which were 1.3-, 1.4- and 1.2-fold superior to foretinib, respectively. The further studies indicated that compound **25s** can induce apoptosis of A549 cells and arrest efficiently the cell cycle distribution in G2/M phase of A549 cells. Moreover, compound **25s** can also inhibit of c-Met phosphorylation in A549 cells by a dose-dependent manner. Collectively, these results indicated that compound **25s** could be a potential anticancer lead compound deserving for further development.

Comprehensive Graphic Content

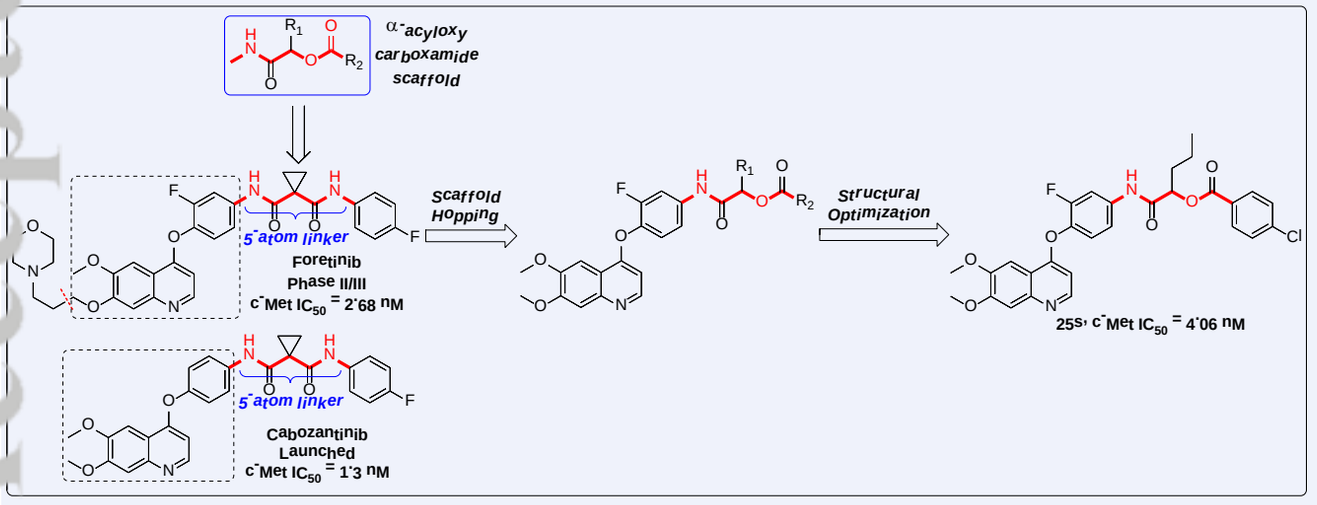

*E-mail: renyulin1104@163.com, liming23547@163.com
‡These authors contributed equally.

Background and Originality Content

Cancer, also termed as malignancy, is the second leading cause of death after cardiovascular diseases and a serious threat to human health worldwide according to WHO.[1,2] It was predicted that total global cancer cases could increase to 22 million per year by 2030,[3] and especially most of the increased cases will be found in devoloping courties and areas. From the microscopic point of view, the uncontrolled growth of abnormal cells is the main feature of initiation and progression of tumorigenesis. Protein kinases (simply referred to herein as kinases) that transfer the terminal phosphate group of ATP to tyrosine, threonine, or serine residues of proteins play fundamental roles in a series of cell processes, including cell growth, differentiation, metastasis, homeostasis, and death, *etc*.[4,5] In view of its central role, protein kinases have been extensively investigated as a major class of targets for drug discovery.[5,6] To the best of our knowledge, the FDA has approved nearly three dozens kinase inhibitors used as molecular targeted therapy for cancer and other diseases.[7,8] Moreover, the success of marketed drugs such as imatinib, trastuzumab, crotinib, cabozantinib and gefitinib, *etc* further validated the critical roles of protein kinases in cancers and its "druggability".[9]

Mesenchymal-epithelial transition factor (c-Met) is a prototype member of a heterodimeric receptor tyrosine kinase subfamily along with macrophage stimulating 1 receptor RON and the only known high-affinity receptor for hepatocyte growth factor/scatter factor (HGF/SF).[10–12] The HGF/c-Met signaling pathway plays important roles in invasive growth during embryo development and postnatal organ regeneration and is strictly controlled in normal cells and only fully active in adults for wound healing and tissue regeneration.[13] Upon activation by HGF, c-MET induces an invasive program consisting of cell proliferation, migration, invasion, and survival that is essential during normal processes. However, aberrant HGF/c-Met signaling is implicated in the development and progression in a variety of human solid cancers such as thyroid cancer, lung cancer, gastric cancer, colorectal cancer, pancreatic cancer, prostate cancers, renal cancer, *etc*.[14,15] Furthermore, the overexpression of either c-Met or HGF has been demonstrated to correlate with poor prognosis and advanced disease stage for cancer patients.[16–18] More importantly, the synergistic effects between c-Met and other receptor tyrosine kinases and cytokines promote aggressive tumor behavior and

For these reasons mentioned above, c-Met and its ligand HGF have become one of the most promising therapeutic targets in the discovery of anticacer drugs for molecular targeted therapies.

Since c-Met was initially identified as the oncogenic fusion Tpr-Met, many strategies based on different mechanisms have been applied to inhibit the HGF/c-Met pathway.[20] Small molecular inhibitors of c-Met tyrosine kinase are hypothesized to be effective for both ligand-dependent and independent activation of c-Met, as such they are the most attractive method for targeting the c-Met pathway.[21,22] Up to now, there have a respectable number of c-Met tyrosine kinase inhibitors (TKIs) currently reaching different clinical stages or being approved as anticancer drugs (**Figure 1**).[23] Among the known c-Met inhibitors, the c-Met TKIs genrally can be categorized into either class I or class II by the virtue of their binding mode in the c-Met kinase domain and structure characteristics.[24,25] According the recent report of c-Met TKIs, many researchers claimed that class II inhibitors may be effective than class I inhibitors for the reasons that class II inhibitors can able to walk away from the gatekeeper and bind with the allosteric site of c-Met.[26] Consequently, a plethora of class II c-Met inhibitors bearing diverse scaffold have been developed. Amongst which the 6,7-disubstituted-4-(2-fluorophenoxy)quinoline scafflod has attracted more and more attention. Moreover, these 6,7-disubstituted-4-phenoxyquinoline derivatives generally have two common structural features in their linkers between moiety B and moiety D, which is known as '5 atoms regulation/hydrogen-bond donors or acceptors' summarized by Gong and co-workers.[27–30] These known structural characteristics suggested that exploration of a suitable linker attached to 6,7-disubstituted-4-phenoxyquinoline scaffold might be a practical way to find more novel class II c-Met inhibitors.

It is worth to note that the expedient synthesis of 5-atom linker is still a significant challenge till now, although great endeavors have been devoted to facilitate the synthesis of the linker between moiety B and moiety D. Multicomponent reactions (MCRs), a powerful chemical tool for the preparation of complex molecules, were virtually deemed to satisfy this criterion that rapid construction of structurally diverse, complex, atom and step economic, high efficient, and chemical libraries of "drug-like"molecules from simple precursors.[31,32] Moreover,

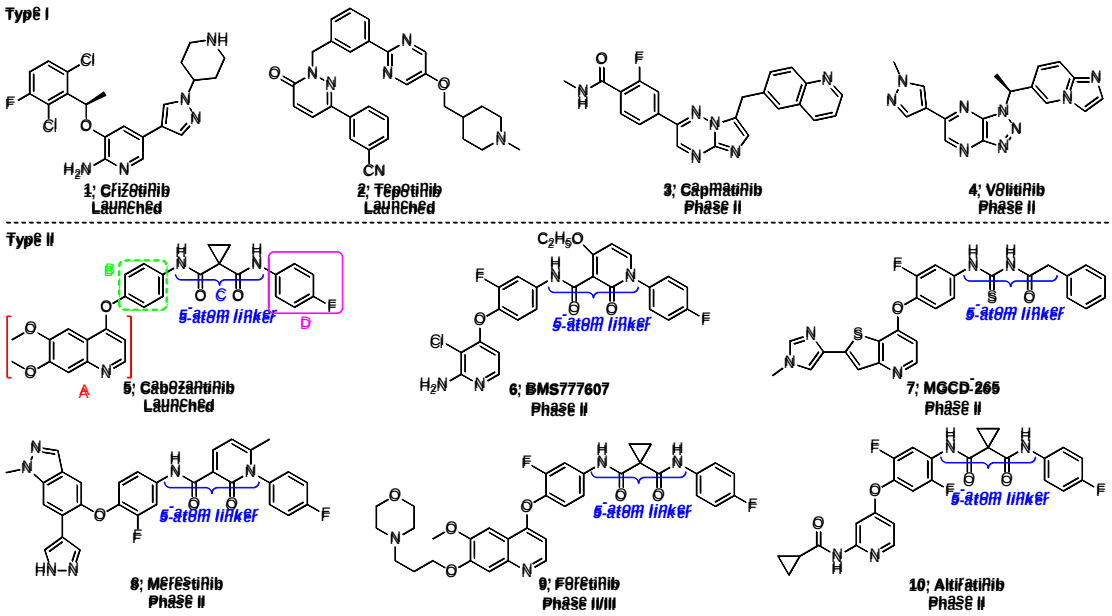

Figure 1 The representative small molecule c-Met kinase inhibitors of different structural types.

) are by far the most useful versity and the number of

accessible compounds.[33,34] Passerini reaction (P-3CR), one of the oldest multicomponent reactions, has been found useful for the construction of multifunctional α-acyloxyamide in a practical process.[35] The α-acyloxycarboxamide linker, a resulting scaffold of Passerini reaction, conformed to the characteristic of the '5-atom regulation' and contained both hydrogen-bond donor and acceptor simultaneously. More importantly, analogs bearing α-acyloxycarboxamide moiety have generally been reported to exhibit diverse biological activities, such as antitumor, antimalarial and antituberculosis, *etc* (**Figure 2**).[36–38] Therefore, we envisioned that the utilization of P-3CR would offer a rapid and effective synthetic strategy for construction of the desired 5-atom linker to facilitate the discovery of structurally novel c-Met inhibitors. Meanwhile, various substituents were introduced into the moiety C and D to investigate the effects on activity. All the target compounds were evaluated for their c-Met kinase inhibitory activity and antiproliferative activities against five cancer cell lines including A549, HT-29, Caki-1, T24 and MDA-MB-231. Moreover, cell apoptosis and cycle arrest, western blot, and kinase selectivity for the representative compound **25s** were further explored. Besides, docking study was also performed. Taken together, all the postive results suggested that **25s** is a potential anticancer lead compound for clinical trials, deserving further development as a promising c-Met inhibitor for the treatment of cancer. Herein, we describe the design, synthesis, and *in vitro* efficacy of this class of compounds in detail.

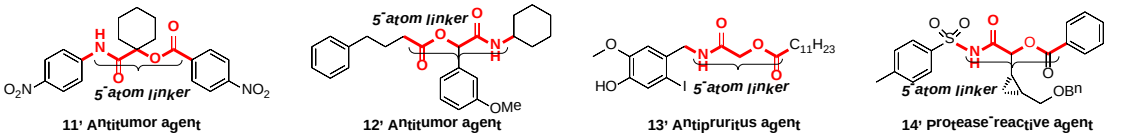

Figure 2 Structures of α-acyloxycarboxamide and selected examples of bioactive molecules.

Results and Discussion

Sytnthesis

As shown in **Scheme 1**, the target compounds were synthesized from commericallly available 4-hydroxy-3-methoxy-acetophenone **15** with a convenient ten-step procedure. The synthesis commenced with a large-scale preparation of the intermediate **24**. Treatment **15** with MeI in the presence of K_2CO_3 afforded disubstituted acetophenone **16** in 91% yield. Regioselective nitration of **16** with concentrated nitric acid proceeded smoothly, furnishing trisubstituted nitro **17** in 82% isolated yield, which underwent aminomethylenation with *N*,*N*-dimethylformamide dimethyl acetal (DMF-DMA) to provide 3-(dimethylamino)-prop-2-en-1-one **18**.[39] Intramolecular cyclization of **18** in the presence of iron powder and acetic acid proceeded smoothly to afford the desired 4-quinolin-ol **19**. Exposure of **19** to $POCl_3$ in the presence of Et_3N gave **20** in 61% yield as a white product. The elaborated chloride **20** underwent a sequence of coupling, reduction, formylation and dehydration to furnish **24** with good overall efficiency as a critical substrate for Passerini reaction. With a large quantity of **24** in hand, we investigated the conditions for its conversion into **25** and the results were summarized in **Table 1**, the target compounds **25a–w** bearing α-acyloxycarboxamide moiety were successfully prepared in moderate to good yield.[40]

In vitro enzymatic assay and structure-activity relationships

All the newly synthesized target compounds **25a–w** were evaluated for their c-Met kinase inhibitory activity *in vitro* using homogeneous time-resolved fluorescence (HTRF) assay. Foretinib, an experimental drug candidate currently in phase II clinical development, was used as a positive control. And the results expressed as the half-maximal inhibitory concentration (IC_{50}) values were summarized in **Table 2**, which was the average of at least three independent experiments.

As described in **Table 2**, these novel 6,7-dimethoxy-4-(2-fluorophenoxy)quinoline derivatives bearing α-acyloxycarboxamide moiety were found to be active against c-Met kinase, showing effeicently inhibitory acitivity at nanomole level with IC_{50} values ranging from 4.06 to 91.52 nM. To our delight, two of them (**25p**, IC_{50} = 6.48 nM; **25s**, IC_{50} = 4.06 nM) showed the most promising acitivity, which was comparable with the reference foretinib. Based on the positive results mentioned above, the introduction of new moiety α-acyloxycarboxamide as the 5-atom linker to 6,7-dimethoxy-4-(2-fluorophenoxy)quinoline

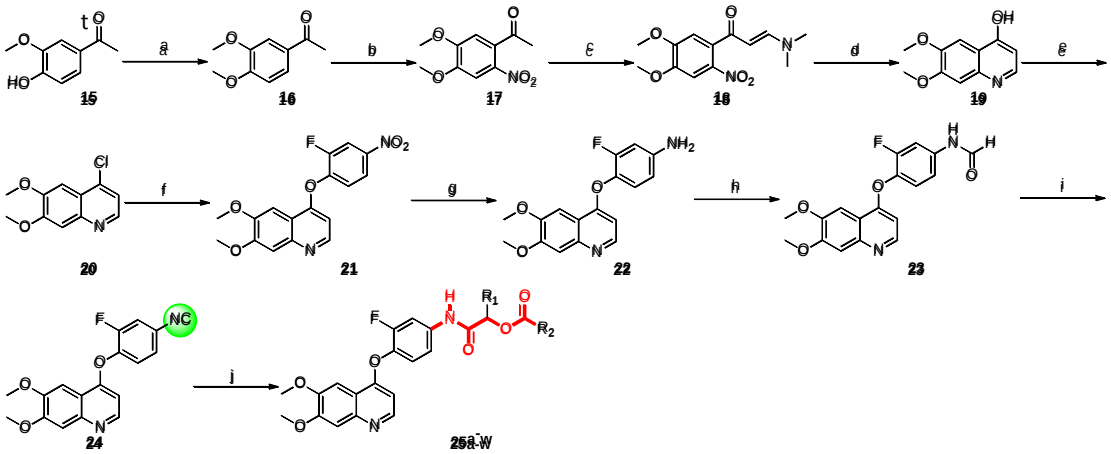

Scheme 1 Reagents and conditions: (a) CH_3I, K_2CO_3, acetone, r.t., 4 h; (b) concentrated nitric acid, 0 °C, overnight; (c) DMF-DMA, toluene, reflux; (d) Fe (powder), AcOH, 80 °C, 2 h; (e) $POCl_3$, reflux, DMF (cat.); (f) 2-fluoro-4-nirophenol, PhCl, 140 °C, 20 h; (g) $SnCl_2{\cdot}2H_2O$, EtOH, 70 °C, 6 h; (h) ethyl formate,

TEA, refluxing, 18 h; (i) $POCl_3$, TEA, $CHCl_3$, 0 °C; (j) THF/H_2O = 3:1, 40 °C, 24 h.

Table 1 Screening of the Passerini reaction conditions.

Entry	Solvent	Con. (M)	Temp. (°C)	Time (h)	Yield (%)
1	DCM	0.1	R.T.	24	0
2	DCE	0.1	R.T.	24	0
3	THF	0.1	R.T.	24	0
4	MeCN	0.1	R.T.	24	0
5	DCM	0.2	R.T.	24	trace
6	DCE	0.2	R.T.	24	trace
7	THF	0.2	R.T.	24	15
8	MeCN	0.2	R.T.	24	11
9	THF	0.4	R.T.	24	28
10	MeCN	0.4	R.T.	24	19
11	THF	0.5	R.T.	24	21
12	THF	0.4	30	24	42
13	THF	0.4	40	24	53
14	THF	0.4	50	24	47
15	THF	0.4	40	48	56
16	THF/H_2O (5/1)	0.4	40	24	65
17	THF/H_2O (3/1)	0.4	40	24	72
18	THF/H_2O (1/1)	0.4	40	24	39

scaffold could maintain the potent c-Met kinase inhibitory activity, simultaneously, suggesting that exploration of a suitable 5-atom linker is still a feasible way to discovery of novel lead compounds for treatment of cancer.

Initially, in view of the central role of 5-atom linker on activity, compounds with diverse R_1 substituents, including phenyl, cyclohexenyl and propyl, were investigated to discover the preliminary structure-activity relationships. Compounds **25a–c** and **25d–e**, in which R_1 was substituted with bulky-group cyclohexyl and electron withdrawing-group phenyl, respectively, only both displayed moderate c-Met kinase inhibitory activity compared with the positive foretinib, which suggested that R_1 was fairly sensitive to both the steric hindrance and electronegativity. Gratifyingly, compounds **25f–h**, R_1 was replaced with *n*-propyl, possessed greater potency than that of compounds **25a–e**, indicating that serving *n*-propyl as the R_1 is more suitable for vander Waals interactions with the backbone of c-Met kinase. As such, *n*-propyl derivatives were further studied in the following work. With the well tolerated group on R_1 (*n*-propyl) in hand, comprehensive *n*-propyl analogs with diverse R_2 substituents, including fifteen aryl rings, an aromatic fused ring, one heterocyclic group and a cyclopentyl, were investigated deeply to discover the structure-activity relationships. The SARs based on IC_{50} values indicated that the R_2 group also played a critical role for c-Met inhibitory efficacy attribute to its essential interactions with the hydrophobic pocket of c-Met. The introduction of cyclopentyl group **25f** (IC_{50} = 53.46 nM) resulted in 3.9-fold loss activity compared with phenyl ring substituted analog **25i** (IC_{50} = 13.65 nM, R_2 = Phenyl), thus indicating that π-aryl interaction virtually plays an essential role in biological activity. To identify potent c-Met inhibitors efficiently, compound **25i** bearing no substituent on phenyl ring was selected as the reference. The introduction of mono-donating groups (mono-EDGs) showed negative tendency in potency such as **25j** (IC_{50} = 18.48 nM, R_2 = 4-Me-Phenyl), **25k** (IC_{50} = 21.83 nM, R_2 = 2,3-$(Me)_2$-Phenyl), **25l** (IC_{50} = 25.43 nM, R = 4-OMe-Phenyl) and **25m** (IC_{50} = 38.35 nM, R_2 = 3,4,5-$(OMe)_3$-Phenyl), which resulted in a 1.4-, 1.6-, 1.9- and 2.8-fold decrease in potency in comparsion with **25i**, respectively. More importantly, the more the number of electron-donating groups and the electron-donating properties, the lower the activities are, exemplified by the preferential order of **25i** > **25j** > **25k** > **25l** > **25m**. In terms of the known results, the investigation of EDGs was not further explored. Inspiringly, the introduction of mono-electron-withdrawing groups (mono-EWGs, such as F and Cl) on phenyl ring showed positive influences on c-Met inhibitory activity. It should be noted that the potency was correlated to the postion of substituent of phenyl, in detail, the mono-EWGs at 4-position of phenyl (**25p**, IC_{50} = 6.48 nM, R = 4-F, increased 2.1-fold) showed more active than that of mono-EWGs at 2-position (**25n**, IC_{50} = 9.32 nM, R = 2-F, increased 1.5-fold) and 3-position of the phenyl (**25o**, IC_{50} = 10.47 nM, R = 3-F, increased 1.3-fold), and the same trend was observed in compounds **25s** > **25q** > **25r**. Moreover, the mono-Cl atom substituted compounds **25q**, **25r**, and **25s** showed superior inhibitory activity than that of same position that was substituted with F atom, repectively. The strong EWG trifluoromethyl substituted analog **25u** (IC_{50} = 41.25 nM, decreased 3.1-fold) displayed obviously decreased activity compared with **25i**, suggesting that the phenyl probably need a proper electron density. The bulky effect of the substituents likely damped the potency, exemplified by the more steric analogues 4-Br-phenyl **25t** (IC_{50} = 20.69 nM, decreased 1.5-fold), 4-(*t*-butyl)-phenyl **25w** (IC_{50} = 20.64 nM, decreased 1.4-fold), and 2-naphthyl **25h** (IC_{50} = 43.36 nM, decreased 3.2-fold) showed obviously decreased activity in comparsion with **25i** (R_2 = Phenyl).

Table 2 In vitro c-Met kinase activities of target compounds **25a–w**.

Compd.	R_1	R_2	c-Met IC_{50} (nM)
25a	Cyclohexyl	Cyclopentyl	68.84 ± 4.65
25b	Cyclohexyl	2-Thienyl	48.43 ± 4.86
25c	Cyclohexyl	2-Naphthyl	54.96 ± 5.85
25d	Phenyl	2-Thienyl	82.45 ± 6.36
25e	Phenyl	2-Naphthyl	91.52 ± 7.38
25f	*n*-Propyl	Cyclopentyl	53.56 ± 4.24
25g	*n*-Propyl	2-Thienyl	32.63 ± 2.72
25h	*n*-Propyl	2-Naphthyl	43.36 ± 3.65
25i	*n*-Propyl	Phenyl	13.65 ± 1.63
25j	*n*-Propyl	4-Me-Phenyl	18.48 ± 2.15
25k	*n*-Propyl	2,3-$(Me)_2$-Phenyl	21.83 ± 1.74
25l	*n*-Propyl	4-OMe-Phenyl	25.43 ± 3.15
25m	*n*-Propyl	3,4,5-$(OMe)_3$-Phenyl	38.45 ± 3.42
25n	*n*-Propyl	2-F-Phenyl	9.32 ± 0.83
25o	*n*-Propyl	3-F-Phenyl	10.47 ± 0.95
25p	*n*-Propyl	4-F-Phenyl	6.48 ± 0.58
25q	*n*-Propyl	2-Cl-Phenyl	8.59 ± 0.75
25r	*n*-Propyl	3-Cl-Phenyl	9.33 ± 1.06
25s	*n*-Propyl	4-Cl-Phenyl	4.06 ± 0.35
25t	*n*-Propyl	4-Br-Phenyl	20.69 ± 1.85
25u	*n*-Propyl	4-CF_3-Phenyl	41.25 ± 2.66
25v	*n*-Propyl	3,4-$(Cl)_2$-Phenyl	10.58 ± 0.87
25w	*n*-Propyl	4-(*t*-Butyl)-Phenyl	20.64 ± 1.89
Foretinib			2.68 ± 0.32

The decreased inhibitory potency might be realted to the hydrophobic pocket of c-Met was not large enough to accommodate with the bulky groups.

In summary, the pharmacological data above of 6,7-dimethoxy-4-(2-fluorophenoxy)quinoline derivatives bearing α-acyloxycarboxamide moiety demonstrated that a favorable linker (R_1 = *n*-Propyl) with proper electronic density and steric hindrance (R_2 = 4-F-Phenyl or 4-Cl-Phenyl) are the main feature for the inhibitory potency of c-Met. Moreover, the pharmacological data demonstrated that the hydrophobic pocket can accommodate the mono-EWGs on phenyl, particularly the mono-EWGs(such as F and Cl) at *para*-position of phenyl ring.

In vitro antiproliferative assays of target compounds against four human tumor cell lines

To further identification the antiproliferative acitivities of these target compounds, MTT assay was used to evaluate the *in vitro* cytotoxicity of compounds **25a–w** against five human tumor cell lines, including three c-Met-addicted cancer cell lines A549 (human lung carcinoma), HT-29 (human colon adenocarcinoma), Caki-1 (human renal cell carcinoma) and two c-Met less-sensitive cell lines, T24 (human bladder transitional cell carcinoma) and MDA-MB-231 (triple-negative human breast cancer), respectively, taking foretinib as a positive control. The antiproliferative activities of target compounds were conducted triplicate experiments and expressed as half-maximal inhibitory concentration (IC_{50}) values listed in **Table 3**.

As shown in **Table 3**, most of the target compounds showed moderate to excellent cytotoxic activities to the five tested tumor cell lines *in vitro*, with IC_{50} values ranging from 0.20 to 19.02 μM. The activity of four target compounds to certain cancer lines was similar or higher than that of foretinib, indicating that the introduction of α-acyloxycarboxamide as '5-atom linker' maintained significant cytotoxicity. Among the substituents of R_1 including *n*-propyl, cyclohexyl and phenyl, higher acitivity was obtained when taking *n*-propyl as R_1, for instance compounds **25f/25a**, **25g/25b/25d** and **25h/25c/25e**. It is worth to note that most of the target compounds displayed remarkable antiproliferative potency against A549 cells, however, the antiproliferative potency against other four cancer cell lines was relatively weak. The most promising compound **25s** exhibited excellent cytotoxicities against A549, HT-29 and MDA-MB-231 with IC_{50} values of 0.39, 0.20, 0.58 μM, respectively, which were 1.2–1.4 folds more active than foretinib. The study on structure-activity relationships (SARs) of antiproliferative acitivity revealed that these target compounds showed a strong parallel correlation between anti-proliferative activity and enzymatic assay: (I) taking *n*-propy as R_1 generally displayed higher potency than other substituents such as cyclohexyl and phenyl; (II) target compounds showed high selectivity toward A549 cells; (III) the EWGs (such as F and Cl) on the moiety D benefited to the potency, and the potency of *para*-substituted phenyl ring (moiety D) was higher than that of *ortho*- and *meta*-substituted; (IV) bulky groups on the phenyl ring (such as Br and *t*-Butyl) led to an obviously decrease in antiproliferative activity; (V) strong/double electron-withdrawing groups led to an obvious decrease in cytotoxicity.

Cell apoptosis and cycle arrest

In view of A549 cell line displayed higher sensitivity than the other four tested cancer cell lines to the target compounds in the preliminary cytotoxicity profile, A549 cells were used in our mechanistic study. To reveal the specific mechanism of antiproliferative potency associated with **25s** on human tumor cells, the effect of **25s** on A-549 cells apoptosis and cells cycle analysis was measured by double staining with FITC-annexin V and propidium iodide and analyzed with flow cytometry. As shown in **Figure 3**, after A549 cells were treated with **25s** at concentrations of 0.25, 0.5 and 1.0 μM for 48 h, the percentage of apoptotic cells was determined to be 14.44%, 28.59% and 34.04%, respectively. Compared with the control group (4.46%), **25s** significantly induced the A549 cells apoptosis in a dose-dependent manner. More importantly, the percentage of total apoptotic cells of **25s** was comparable with foretinib (**25s** *vs* **foretinib**, 34.04% *vs* 34.15%) at the same concentration of 1.0 μM and the early apoptotic of **25s** was superior than that of foretinib (**25s** *vs* **foretinib**, 21.60% *vs* 11.25%). We then investigated the effect of **25s** on blocking cell cycle progression in A549 cells. As shown in **Figure 4**, after treatment of compound **25s** with different concentration, the percentage of cells in G2/M phase remarkably increased in a dose-dependent manner compared with the control group, which was similar with the effect of foretinib on A549 cells. On the whole, these results demonstrated that **25s** induced cell cycle arrest at G2/M phase and led to cellular apoptosis in A549 cells.

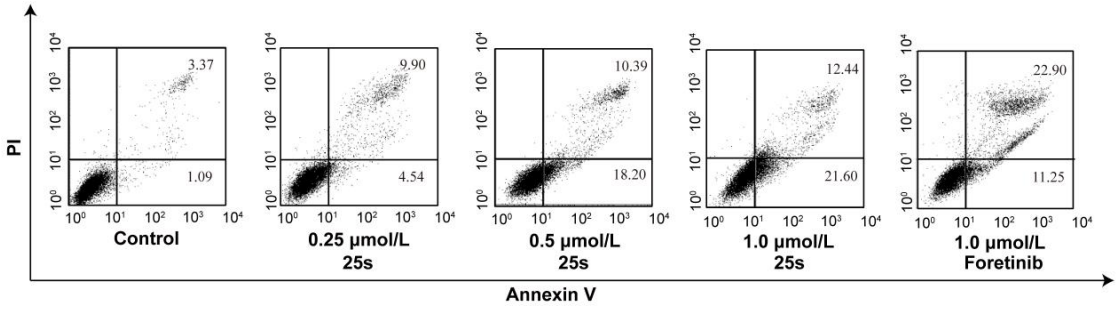

Figure 3 The effect of **25s** on A549 cells apoptosis by Annexin-FITC/PI double staining.

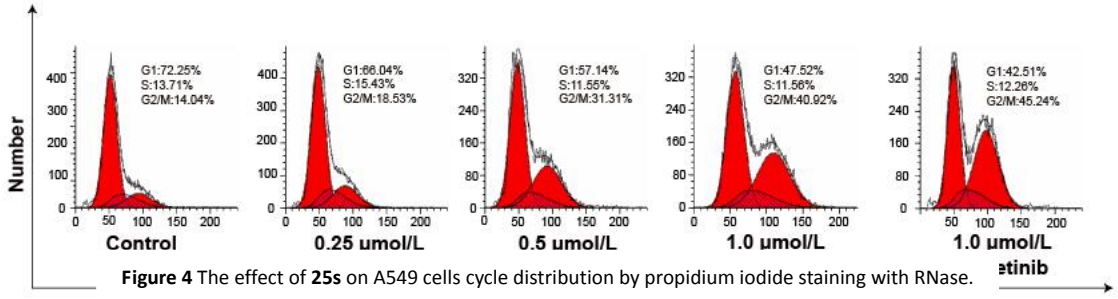

Figure 4 The effect of **25s** on A549 cells cycle distribution by propidium iodide staining with RNase.

Table 3 In vitro cytotoxicity data for **25a–w** against five selected human tumor cell lines.

Compd.	R_1	R_2	IC_{50} (μmol/L) ± SD				
			A549	HT-29	Caki-1	T24	MDA-MB-231
25a	Cyclohexyl	Cyclopentyl	8.48 ± 0.92	9.35 ± 1.03	13.35 ± 0.96	ND	ND
25b	Cyclohexyl	2-Thienyl	6.56 ± 0.54	7.47 ± 0.48	10.26 ± 0.89	14.26 ± 1.35	8.26 ± 0.94
25c	Cyclohexyl	2-Naphthyl	7.34 ± 0.65	8.26 ± 0.73	11.68 ± 1.05	16.86 ± 1.58	11.68 ± 0.96
25d	Phenyl	2-Thienyl	10.37 ± 1.18	11.46 ± 1.25	15.45 ± 1.28	18.45 ± 0.96	17.75 ± 1.57
25e	Phenyl	2-Naphthyl	12.86 ± 1.05	15.65 ± 1.75	17.13 ± 0.84	17.95 ± 1.24	ND
25f	*n*-Propyl	Cyclopentyl	6.08 ± 0.56	7.06 ± 0.58	10.02 ± 0.93	13.23 ± 1.13	8.15 ± 0.72
25g	*n*-Propyl	2-Thienyl	3.85 ± 0.43	4.57 ± 0.39	6.23 ± 0.58	8.59 ± 0.62	7.52 ± 0.65
25h	*n*-Propyl	2-Naphthyl	4.53 ± 0.56	5.66 ± 0.62	5.89 ± 0.46	9.38 ± 0.75	6.89 ± 0.58
25i	*n*-Propyl	Phenyl	0.96 ± 0.13	1.35 ± 0.14	3.63 ± 0.37	6.05 ± 0.57	2.66 ± 0.25
25j	*n*-Propyl	4-Me-Phenyl	1.55 ± 0.16	2.08 ± 0.18	4.58 ± 0.53	6.68 ± 0.72	3.73 ± 0.42
25k	*n*-Propyl	2,3-$(Me)_2$-Phenyl	1.96 ± 0.18	2.74 ± 0.23	5.36 ± 0.49	7.36 ± 0.63	5.85 ± 0.63
25l	*n*-Propyl	4-OMe-Phenyl	2.85 ± 0.23	4.05 ± 0.36	6.48 ± 0.76	8.59 ± 0.64	6.46 ± 0.54
25m	*n*-Propyl	3,4,5-$(OMe)_3$-Phenyl	4.64 ± 0.38	7.23 ± 0.65	8.06 ± 0.72	8.37 ± 0.59	8.59 ± 0.75
25n	*n*-Propyl	2-F-Phenyl	0.63 ± 0.07	0.85 ± 0.10	3.18 ± 0.29	4.46 ± 0.52	1.88 ± 0.23
25o	*n*-Propyl	3-F-Phenyl	0.76 ± 0.08	0.84 ± 0.13	3.06 ± 0.45	4.68 ± 0.49	2.34 ± 0.18
25p	*n*-Propyl	4-F-Phenyl	0.55 ± 0.05	0.68 ± 0.12	2.85 ± 0.19	4.05 ± 0.38	1.37 ± 0.12
25q	*n*-Propyl	2-Cl-Phenyl	0.59 ± 0.06	0.76 ± 0.11	2.66 ± 0.21	3.94 ± 0.26	1.69 ± 0.13
25r	*n*-Propyl	3-Cl-Phenyl	0.68 ± 0.08	0.94 ± 0.15	2.73 ± 0.15	4.15 ± 0.30	2.06 ± 0.16
25s	*n*-Propyl	4-Cl-Phenyl	0.39 ± 0.05	0.20 ± 0.03	2.35 ± 0.33	3.46 ± 0.25	0.58 ± 0.07
25t	*n*-Propyl	4-Br-Phenyl	1.74 ± 0.18	2.36 ± 0.19	4.95 ± 0.38	6.26 ± 0.55	4.25 ± 0.36
25u	*n*-Propyl	4-CF_3-Phenyl	13.18 ± 1.25	15.46 ± 1.18	19.02 ± 0.94	16.35 ± 1.18	ND
25v	*n*-Propyl	3,4-$(Cl)_2$-Phenyl	0.88 ± 0.09	1.06 ± 0.14	3.06 ± 0.46	4.52 ± 0.36	2.16 ± 0.15
25w	*n*-Propyl	4-(*t*-Butyl)-Phenyl	2.08 ± 0.16	2.96 ± 0.22	5.23 ± 0.45	8.85 ± 0.69	4.16 ± 0.39
Foretinib			0.46 ± 0.05	0.28 ± 0.03	2.12 ± 0.28	3.15 ± 0.19	0.70 ± 0.06

Western blotting analysis of c-Met

With a large-scale results of the cell-biochemical and cell-proliferation assay in hand, **25s** was proven to be a potent c-Met inhibitor. To further assess whether downregulate c-Met kinase activation of **25s** in a cell-free system can be recapitulated *in vitro*, western blotting assay was carried out to determine the effect of **25s** on phosphorylation of c-Met in living cells. A549 cells were treated with **25s** at different concentration (1.0, 2.0 and 4.0 μM) and DMSO as negative control for 24 h, and the level of GAPDH served as loading control. As depicted in **Figure 5**, compound **25s** inhibited c-Met phosphorylation in a dose-dependent manner that consistents with the observed *in vitro* activity, suggesting that the antiproliferative activity of **25s** might be, or at least partially, through inhibiting the activation of c-Met.

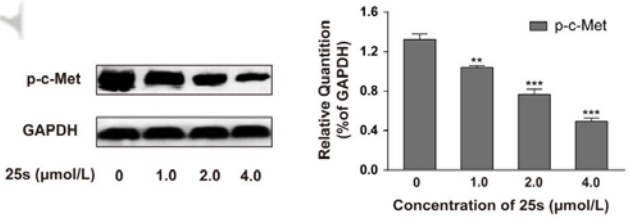

Figure 5 Inhibition of c-Met phosphorylation by the privileged compound **25s** in A549 cells.

In vitro kinase profile

Table 4 Kinase selectivity profile of compound **25s** and **Foretinib**.

Enzyme	Enzyme IC_{50} (nM)	
	25s	**Foretinib**
c-kit	8.16	7.23
PDGFRα	425	4.52
PDGFRβ	548	8.96
Ron	10.65	4.14
VEGFR-2	752	5.45
EGFR	>10,000	3050
Flt-3	11.58	5.86
ALK	>10,000	>5,000
Flt-4	476	4.48
c-Met	4.06	2.64

With any kinase inhibitor, understanding the off-target kinase inhibition is crucial, particularly to help explain both efficacy and potential side effects. In view of its remarkable potency against c-Met kinase, the most promising compound **25s** was selected to further screen against a panel of kinases, including c-Met family member Ron, highly homologous kinase ALK and other 7 tyrosine kinases. As shown in **Table 4**, compared with its high potency against c-Met (IC_{50} = 4.06 nM), **25s** also exhibited high inhibitory effects against c-kit (IC_{50} = 8.16 nM), Ron (IC_{50} = 10.65 nM) and

Flt-3 (IC_{50} = 11.58 nM). In contrast to its high potency against c-Met kinase, **25s** showed much weaker inhibition against PDGFRα, PDGFRβ, VEGFR-2 and Flt-4, the potency was 105-, 135-, 185-, and 117-fold lower than against c-Met, respectively. In addition, **25s** exhibited a slight or no tyrosine kinase inhibitory activity against EGFR (IC_{50} > 10 μM) and ALK (IC_{50} > 10 μM). Taken together, these data suggested that compound **25s** is a promising multitarget inhibitor of tyrosine kinase, indicating **25s** might act through multiple mechanisms rather than only by inhibiting c-Met kinase. Further studies on the mechanism of these compounds are in progress and will report in due course.

Molecular docking study of compound 25s

To further explore the binding mode of target compounds with the active site of c-Met, molecular docking simulation studies were carried out by using Autodock 4.2 package. Based on the *in vitro* inhibition results, we selected compound 10m, the best c-Met inhibitor in this study, as ligand example, and the structure of c-Met was selected as the docking model (PDB ID code: 3LQ8). The binding modes of compound **25s** and c-Met was shown in **Figure 6**, and the nitrogen atom of quinoline, the hydrogen atom of α-acyloxycarboxamide moiety in compound **25s** formed two H-bond interactions with protein residue Met1160 and Asp1222, respectively. At the same time, one π-π interaction between the phenyl ring and the Phe1223 has been formed. Moreover, the terminal 4-fluorophenyl ring fitted into the hydrophobic pocket that was formed Phe1134, Met1131, val1155 and Leu1157, *etc*. In general, these results of the molecular docking study showed that 4-phenoxyquinoline derivatives containing α-acyloxycarboxamide moiety could act synergistically to interact with the binding site of c-Met, suggesting that α-acyloxycarboxamide moiety could serve as a promising linker from which to build novel series of c-Met inhibitors.

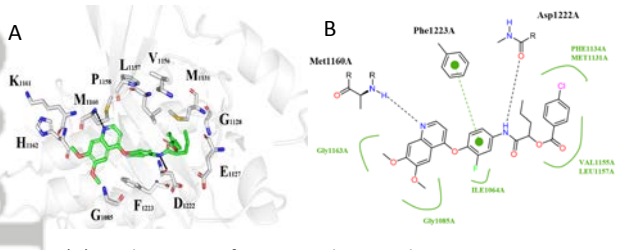

Figure 6 (**A**) Binding pose of compound **25s** with c-Met active site. Compound **25s** was showed in colored sticks, green: carbon atom, blue: nitrogen atom, pink: oxygen atom. (**B**) The interaction details between compound **25s** and c-Met.

PK and LogP profile of compound 25s

As a promising antitumor lead compound, the compound should better has great physicochemical properties. As such, the water-solubility and LogP value were tested. Water-solubility of **25s** (5.03 μg/mL) was significantly greater than the positive foretinib (< 0.1 μg/mL), and the LogP value (2.58) was less than foretinib (3.64). The physicochemical properties results indicated **25s** had good fat-water distribution. Collectively, compound **25s** was demonstrated suitable for being an excellent anticancer lead compound.

Conclusions

In summary, a series of 6,7-disubstituted-4-(2-fluorophenoxy) quinoline derivatives bearing α-acyloxycarboxamide moiety were designed, synthesized *via* Passerini reaction as a key step, and evaluated for their in vitro biological activities against c-Met kinase and five cancer cell lines (A549, HT-29, Caki-1, T24, and MDA-MB-231). To our delight, most of the target compounds displayed moderate-to-excellent activity against c-Met and selected cancer cells. It is worth to note that the target compounds displayed remarkable antiproliferative potency against A549 cells. The preliminary SARs studies indicated that the introduction of α-acyloxycarboxamide as the 5-atom linker maintained the potent activity. In particular, the most promising compound **25s** (c-Met IC_{50} = 4.06 nM) demonstrated excellent c-Met inhibitory activity and remarkable cytotoxicities against A549, HT-29 and MDA-MB-231 with IC_{50} values of 0.39, 0.20, and 0.58 μM, which were 1.3-, 1.4- and 1.2-fold superior to positive foretinib, respectively. After the preliminary screening, **25s** was identified as the most potent c-Met inhibitor of this series analogs at both the enzyme-based and cell-based assay compared with foretinib. The cell cycle and apoptosis results proved that compound **25s** exhibited a significant antiproliferative effect on A549 cells in a does-dependent manner. Moreover, docking study revealed the common mode of **25s** interacted with the c-Met binding site. Taken together, these positive results mentioned above highlight that **25s** is a potential antitumor candidate, deserving further investigation and development. Moreover, further studies on SARs and mechanism of action of these target compounds are currently underway in our laboratory, and the results will be reported in due course.

Experimental

Instruments and materials

All common reagents and materials were purchased from commercial sources and were used without further purification. Organic solvents were routinely dried and/or distilled prior to use and stored over molecular sieves under argon. Organic extracts were, in general, dried over anhydrous sodium sulfate (Na_2SO_4). TLC plates were visualized by exposure to ultra violet light (UV). Column chromatography was run on silica gel (200–300 mesh) from Qingdao Ocean Chemicals (Qingdao, Shandong, China). Mass spectra were recorded on a BrukerDaltonics APEXII49e spectrometer with ESI source as ionization. Melting points were measured by using a Gongyi X-5 microscopy digital melting point apparatus and are uncorrected. ^{1}H NMR and ^{13}C NMR spectra were obtained by using a Bruker Advance III 400 MHz NMR spectrometer with TMS as an internal standard. Data are represented as follows: chemical shift, multiplicity (s = singlet, d = doublet, t = triplet, q = quartet, m = multiplet, br = broad), integration, and coupling constant in Hertz (Hz). Unless otherwise noted, all yields are unoptimized and generally represent the result of a single experiment.

General synthetic procedure for target compounds 25a–w

To a stirred solution of aldehyde/ketone (0.4 mmol) in THF/H_2O (0.5 mL, v/v = 3:1) was added carboxylic acid (0.4 mmol) and **24** (0.2 mmol) at room temperature. Subsequently, the reaction mixture was heated at 40 °C for 24 h. After completion of the reaction (TLC monitoring), the mixture was cooled to room temperature and solvent was evaporated. The residue was purified by chromatography on silica gel using ethyl acetate/*n*-hexane as eluent to afford the target compounds **25a–w**.

Cytotoxicity against tumor cells assay

The cancer cells were cultured in minimum essential medium (MEM) supplemented with 10% fetal bovine serum (FBS). Approximately 4 × 10^3 cells per well, suspended in MEM medium, were plated onto each well of a 96-well plate and incubated in 5% CO_2 at 37 °C for 24 h. The test compounds were added to the culture medium at the indicated final concentrations and the cell cultures were continued for 72 h. Fresh MTT was added to each well at a final concentration of 5 μg/mL and incubated with cells at 37 °C for 4 h. The formazan crystals were dissolved in 100 μL of DMSO per each well, and the absorbency at 492 nm (for the

absorbance of MTT formazan) and 630 nm (for the reference wavelength) was measured with the ELISA reader. All compounds were tested three times in each of the cell lines. The results expressed as IC_{50} (inhibitory concentration of 50%) were the average of three determinations calculated by using the Bacus Laboratories Incorporated Slide Scanner (Bliss) software.

Tyrosine kinases assay

The tyrosine kinases activities were evaluated using homogeneous time-resolved fluorescence (HTRF) assays, as previously reported protocol.[41] Briefly, 20 mg/mL poly (Glu, Tyr) 4:1 (Sigma) was preloaded as a substrate in 384-well plates. Then 50 μL of 10 mM ATP (Invitrogen) solution diluted in kinase reaction buffer (50 mM HEPES, pH 7.0, 1 M DTT, 1 M $MgCl_2$, 1 M $MnCl_2$, and 0.1% NaN_3) was added to each well. Various concentrations of compounds diluted in 10 μL of 1% DMSO (v/v) were used as the negative control. The kinase reaction was initiated by the addition of purified tyrosine kinase proteins diluted in 39 μL of kinase reaction buffer solution. The incubation time for the reactions was at 25 °C for 30 min, and the reactions were stopped by the addition of 5 μL of Streptavidin-XL665 and 5 μL of Tk Antibody Cryptate working solution to all of wells. The plates were read using Envision (PerkinElmer) at 320 nm and 615 nm. The inhibition rate (%) was calculated using the following equation: % inhibition 100 = [(Activity of enzyme with tested compounds-Min)/(Max-Min)] × 100 (Max: the observed enzyme activity measured in the presence of enzyme, substrates, and cofactors; Min: the observed enzyme activity in the presence of substrates, cofactors and in the absence of enzyme). IC_{50} values were calculated from the inhibition curves.

Analysis of cellular apoptosis

Apoptosis was detected by an Annexin V-FITC/propidium iodide double staining kit (BD Biosciences) since AnnexinV-fluorescein isothiocyanate (Annexin V-FITC) is a protein that possesses high affinity to phosphatidyl serine PS, which can be detected by staining with Annexin V-FITC and counter staining with propidium iodide (PI). A549 cells were seeded in 6-well plates and allowed to grow for 24 h in culture medium and then treated with vehicle, 1.0 μM of foretinib, 0.25, 0.5 and 1.0 μM of **25s**. The cells were incubated at 37 °C, 5% CO_2 for 12 h. Cells were harvested by centrifugation at 2000 r/min for 5 min and washed with iced PBS solution. The supernatant was abandoned and 195 μL of Annexin V-FITC binding buffer solution (10 mM HEPES, 140 mM NaCl, and 2.5 mM $CaCl_2$ at pH 7.4) was added to resuspend the cells. Afterwards, 5 μL of Annexin V-FITC and 10 μL of propidium iodide staining solution were added and the solution was mixed gently. Next, these samples were incubated in dark at room temperature for 30 min and the labeled cells were analyzed by flow cytometer (FACScan, Bection Dickinson).

Flow cytometric analysis of cell cycle distribution

Cell cycle analysis was carried out through flow cytometer. A549 cells were seeded in 6-well plates (3×10^5 cells/well), incubated in the presence or absence of **25s** and foretinib at the indicated concentrations at 37 °C for 24 h, 5% CO_2. Cells were washed twice with phosphate buffer saline, harvested by centrifugation and then fixed in ice-cold 70% ethanol overnight. After the ethanol was removed the next day, the cells were resuspended in ice-cold PBS, treated with RNase A (Keygen Biotech, China) at 37 °C for 30 min, and then incubated with the DNA staining solution propidium iodide (PI, Keygen Biotech, China) at 4 °C for 30 min. DNA cell cycle profiling was determined by measuring DNA content by using flow cytometer (FACScan, Bection Dickinson), and the percentage of G1, S, G2/M cells was calculated by using ModFit LT version 3.0.

Western Blotting analysis

A549 cells were cultured under regular growth conditions to the exponential growth phase. Then A549 cells (5.0×10^5 cells/dish) were incubated with or without **25s** at various concentrations for 6 h. After incubation, the cells were collected by centrifugation and washed twice with phosphate-buffered saline chilled to 0 °C. The cells were homogenized in RIPA lysis buffer containing 150 mM NaCl, 50 mM Tris (pH 7.4), 1% (w/v) sodium deoxycholate, 1% (v/v) Triton X-100, 0.1% (w/v) SDS, and 1 mM EDTA (Beyotime, China). The lysates were incubated on ice for 30 min, intermittently vortexed every 5 min, and centrifuged at 12 500 g for 15 min to harvest the supernatants. Next, the protein concentrations were determined by a BCA Protein Assay Kit (Thermo Fisher Scientific, Rockford, Illinois, USA). The protein extracts were reconstituted in loading buffer containing 62 mM Tris-HCl, 2% SDS, 10% glycerol, and 5% β-mercaptoethanol (Beyotime, China), and the mixture was boiled at 100 °C for 10 min. An equal amount of the proteins (50 mg) was separated by 8–12% sodium dodecyl sulfate-polyacrylamide gel electrophoresis (SDS-PAGE) and transferred to nitrocellulose membranes (Amersham Biosciences, Little Chalfont, Buckinghamshire, UK). Then, the membranes were blocked with 5% nonfat dried milk in TBS containing 1% Tween-20 for 90 min at room temperature and were incubated overnight with specific primary antibodies (CST, USA) at 4 °C. After washing three times with TBS, the membranes were incubated with the appropriate HRP-conjugated secondary antibodies at room temperature for 2 h. The blots were developed with enhanced chemiluminescence (Pierce, Rockford, Illinois, USA) and were detected by an LAS4000 imager (GE Healthcare, Waukesha, Wisconsin, USA).

Molecular docking

For docking purposes, the three-dimensional structure of the c-Met (PDB code: 3LQ8) were obtained from RCSB Protein Data Bank.[42] Hydrogen atoms were added to the structure allowing for appropriate ionization at physiological pH. The protonated state of several important residues, such as CYS919, and ASP1046 were adjusted by using SYBYL 6.9.1 (Tripos, St. Louis, USA) in favor of forming reasonable hydrogen bond with the ligand. Molecular docking analysis was carried out by the Autodock 4.2 package to explore the binding model for the active site of c-Met with its ligand. All atoms located within the range of 5.0 Å from any atom of the cofactor were selected into the active site, and the corresponding amino acid residue was, therefore, involved into the active site if only one of its atoms was selected. Other parameters were all set as default in the docking calculations. All calculations were performed on Silicon Graphics workstation.

PK and LogP profile assays

The water-solubility of **25s** was determined by ultrasonic method. Excess solid was added into 1 mL of ultra-pure water, and sonicated for 1 h, after stewing, 10 mL of the sample filtrated with 0.25 mm microporous membrane was injected and analyzed, then the peak area was measured, water solubility of the compounds could also be calculated according to the standard curve. Meanwhile, like the water-solubility assays, LogP was measured subsequently. Excess solid was added into 0.6 mL of ultra-pure water and 0.6 mL *n*-octanol, repeat vortexed 2 min and sonicated for 30 min twice, and centrifuged (3000 rmp, 5 min) to separate the aqueous phase and organic phase. The organic phase was diluted 10 times and filtrated with 0.25 mm microporous membrane, then did as the process in water-solubility assays. The LogP value of **25s** was calculated using the formula below: LogP = Log(peak area organic phase/peak area aqueousphase).

Supporting Information

The supporting information for this article is available on the WWW under https://doi.org/10.1002/cjoc.2021xxxxx.

Acknowledgement

This work was supported by the Fundamental Research Funds for the Central Universities (31920170193, 31920200026).

References

[1] http://www.who.int/mediacentre/factsheets/fs297/en/, 2017.
[2] Torre, L. A.; Bray, F.; Siegel, R. L.; Ferlay, J.; Lortet-Tieulent, J.; Jemal, A. Global cancer statistics, *CA Cancer J. Clin*. **2015**, *65*, 87–108.
[3] Bray,F.; Jemal, A.; Grey, N.; Ferlay, L.; Forman, D. Global cancer transitions according to the Human Development Index (2008–2030): a population-based study. *Lancet Oncol*. **2012**, *13*, 790–801.
[4] Manning, G.; Whyte, D. B.; Martinez, R.; Hunter, T.; Sudarsanam, S. The protein kinase complement of the human genome. *Science* **2002**, *298*, 1912–1934.
[5] Wang, Z.; Cole, P. A. Catalytic mechanisms and regulation of protein kinases. *Methods Enzymol*. **2014**, *548*, 1–21.
[6] Lu, X; Smaill, J. B.; Ding, K. Medicinal chemistry strategies for the development of kinase inhibitors targeting point mutations. *J. Med. Chem*. **2020**, *63*, 10726–10741.
[7] Wu, P.; Nielsen, T. E.; Clausen, M. H. Small molecule kinase inhibitors: an analysis of FDA-approved drugs. *Drug Discovery Today* **2016**, *21*, 5–10.
[8] Wu, P.; Nielsen, T. E.; Clausen, M. H. FDA-approved small molecule kinase inhibitors. *Trends Pharmacol. Sci*. **2015**, *36*, 422–439.
[9] Cui, J. J. Targeting receptor tyrosine kinase MET in cancer: small molecule inhibitors and clinical progress. *J. Med. Chem*. **2014**, *57*, 4427–4453.
[10] Dean, M.; Park, M.; Le Beau, M. M.; Robins, T. S.; Diaz, M. O.; Rowley, J. D.; Blair, D. G.; Vande Woude, G. F. The human *met* oncogene is related to the tyrosine kinase oncogenes. *Nature* **1985**, *318*, 385–388.
[11] Bottaro, D.P.; Rubin, J. S.; Faletto, D. L.; Chan, A. M. -L.; Kmiecik, T. E.; Vande Woude, G. F.; Aaronson, S. A. Identification of the hepatocyte growth factor receptor as the c-*met* proto-oncogene product. *Science* **1991**, *251*, 802–804.
[12] Robinson, D. R.; Wu, Y. -M.; Lin, S. -F. The protein tyrosine kinase family of the human genome. *Oncogene* **2000**, *19*, 5548–5557.
[13] Trusolino, L.; Comoglio, P. M. Scatter-factor and semaphorin receptors: cell signaling for invasive growth. *Nat. Rev. Canc.* **2002**, *2*, 289–300.
[14] Birchmeier, C.; Birchmeier, W.; Gherardi, E.; Vande Woude, G. F. Met, metastasis, motility and more. *Nat. Rev. Mol. Cell Biol.* **2003**, *4*, 915–925.
[15] Gao, W.; Han, J. Overexpression of ING5 inhibits HGF-induced proliferation, invasion and EMT in thyroid cancer cells *via* regulation of the c-Met/PI3K/Akt signaling pathway. *Biomed. Pharmacother*. **2018**, *98*, 265–270.
[16] Takayama, H.; LaRochelle, W. J.; Sharp, R.; Otsuka, T.; Kriebel, P.; Anver, M.; Aaronson, S. A.; Merlino, G. Diverse tumorigenesis associated with aberrant development in mice overexpressing hepatocyte growth factor/scatter factor. *Proc. Natl. Acad. Sci. USA* **1997**, *94*, 701–706.
[17] Baldacci, S.; Kherrouche, Z.; Cockenpot, V.; Stoven, L.; Copin, M. C.; Werkmeister, E.; Marchand, N.; Kyheng, M.; Tulasne, D.; Cortot, A. B. *MET* amplification increases the metastatic spread of EGFR-mutated NSCLC. *Lung Cancer* **2018**, *125*, 57–67.
[18] Tsakonas, G.; Botling, J.; Micke, P.; Rivard, C.; LaFleur, L.; Mattsson, J.; Boyle, T.; Hirsch, F. R.; Ekman, S. c-MET as a biomarker in patients with surgically resected non-small cell lung cancer. *Lung Cancer* **2019**, *133*, 69–74.
[19] Tao, L.; Qiu, J.; Slavin, S.; Ou, Z.; Liu, Z.; Ge, J.; Zuo, L.; Guancial, E. A.; Messing, E. M.; Chang, C.; Yeh, S. Recruited T cells promote the bladder cancer metastasis *via* up-regulation of the estrogen receptor β/IL-1/c-MET signals. *Cancer Lett*. **2018**, *430*, 215–223.
[20] D'Angelo, N. D.; Bellon, S. F.; Booker, S. K.; Cheng, Y.; Coxon, A.; Dominguez, C.; Fellows, I.; Hoffman, D.; Hungate, R.; Kaplan-Lefko, P.; Lee, M. R.; Li, C.; Liu, L.; Rainbeau, E.; Reider, P. J.; Rex, K.; Siegmund, A.; Sun, Y.; Tasker, A. S.; Xi, N.; Xu, S.; Yang, Y.; Zhang, Y.; Burgess, T. L.; Dussault, I.; Kim, T. -S. Design, Synthesis, and Biological Evaluation of Potent c-Met Inhibitors. *J. Med. Chem.* **2008**, *51*, 5766–5779.
[21] Wang, W.; Xu, S.; Du, Y.; Liu, X.; Li, X.; Wang, C.; Zhao, B.; Zheng, P.; Zhu, W. Synthesis and bioevaluation and doking study of 1H-pyrrolo[2,3-*b*] pyridine derivatives bearing aromatic hydrazone moiety as c-Met inhibitors. *Eur. J. Med. Chem*. **2018**, *145*, 315–327.
[22] Liu, J.; Gong, Y.; Shi, J.; Hao, X.; Wang, Y.; Zhou, Y.; Hou, Y.; Liu, Y.; Ding, S.; Chen, Y. Design, synthesis and biological evaluation of novel N-[4-(2-fluorophenoxy)pyridin-2-yl]cyclopropanecarboxamide derivatives as potential c-Met kinase inhibitors. *Eur. J. Med. Chem*. **2020**, *194*, 112244.
[23] Parikh, P. K.; Ghate, M. D. Recent advances in the discovery of small molecule c-Met Kinase inhibitors. *Eur. J. Med. Chem*. **2018**, *143*, 1103–1138.
[24] Yuan, H.; Liu, Q.; Zhang, L.; Hu, S.; Chen, T.; Li, H.; Chen, Y.; Xu, Y.; Lu, T. Discovery, optimization and biological evaluation for novel c-Met kinase inhibitors. *Eur. J. Med. Chem*. **2018**, *143*, 491–502.
[25] Nan, X.; Li, H. -J.; Fang, S. -B.; Li, Q. -Y.; Wu, Y. -C. Structure-based discovery of novel 4-(2-fluorophenoxy)quinoline derivatives as c-Met inhibitors using isocyanide-involved multicomponent reactions. *Eur. J. Med. Chem*. **2020**, *193*, 112241.
[26] Zhuo, L. -S.; Xu, H. -C.; Wang, M. -S.; Zhao, X. -E.; Ming, Z. -H.; Zhu, X. -L.; Huang, W.; Yang, G. -F. 2,7-Naphthyridinone-based MET kinase inhibitors: a promising novel scaffold for antitumor drug development. *Eur. J. Med. Chem*. **2019**, *178*, 705–714.
[27] Liu, J.; Yang, D.; Yang, X.; Nie, M.; Wu, G.; Wang, Z.; Li, W.; Liu, Y.; Gong, P. Design, synthesis and biological evaluation of novel 4-phenoxyquinoline derivatives containing 3-oxo-3,4-dihydroquinoxaline moiety as c-Met kinase inhibitors. *Bioorg. Med. Chem*. **2017**, *25*, 4475–4486.
[28] Liao, W.; Xu, C.; Ji, X.; Hu, G.; Ren, L.; Liu, Y.; Li, R.; Gong, P.; Sun, T. Design and optimization of novel 4-(2-fluorophenoxy)quinoline derivatives bearing a hydrazone moiety as c-Met kinase inhibitors. *Eur. J. Med. Chem*. **2014**, *87*, 508–518.
[29] Zhou, S.; Ren, J.; Liu, M.; Ren, L.; Liu, Y.; Gong, P. Design, synthesis and pharmacological evaluation of 6,7-disubstituted-4-phenoxyquinoline derivatives as potential antitumor agents. *Bioorg. Chem*. **2014**, *57*, 30–42.
[30] Zhou, S.; Liao, H.; He, C.; Dou, Y.; Jiang, M.; Ren, L.; Zhao, Y.; Gong, P. Design, synthesis and structure-activity relationships of novel 4-phenoxyquinoline derivatives containing pyridazinone moiety as potential antitumor agents. *Eur. J. Med. Chem*. **2014**, *83*, 581–593.
[31] Dömling, A. Recent developments in isocyanide based multicomponent reactions in applied chemistry. *Chem. Rev*. **2006**, *106*, 17–89.
[32] Dömling, A.; Wang, W.; Wang, K. Chemistry and biology of multicomponent reactions. *Chem. Rev*. **2012**, *112*, 3083–3135.
[33] Kou, L.; Wang, M. -J.; Wang, L. -T.; Zhao, X. -B.; Nan, X.; Yang, L.; Liu, Y. -Q.; Morris-Natschke, S. L.; Lee, K. -H. Toward synthesis of third-generation spin-labeled podophyllotoxin derivatives using isocyanide multicomponent reactions. *Eur. J. Med. Chem*. **2014**, *75*, 282–288.
[34] Zhao, X. -B.; Wu, D.; Wang, M. -J.; Goto, M.; Morris-Natschke, S. L.; Liu, Y. -Q.; Wu, X. -B.; Song, Z. -L.; Zhu, G. -X.; Lee, K. -H. Design and synthesis of novel spin-labeled camptothecin derivatives as potent cytotoxic agents. *Bioorg. Med. Chem*. **2014**, *22*, 6453–6458.
[35] Zhang, J.; Lin, S. -X.; Cheng, D. -J.; Liu, X. -Y.; Tan, B. Phosphoric acid-catalyzed asymmetric classic passerini reaction. *J. Am. Chem. Soc.* **2015**, *137*, 14039–14042.
[36] Serafini, M.; Griglio, A.; Aprile, S.; Seiti, F.; Travelli, C.; Pattarino, F.; Grosa, G.; Sorba, G.; Genazzani, A. A.; Gonzalez-Rodriguez, S.; Butron, L.; Devesa, I.; Fernandez-Carvajal, A.; Pirali, T.; Ferrer-Montiel, A. Targeting transient receptor potential vanilloid 1 (TRPV1) channel

softly: the discovery of passerini adducts as a topical treatment for inflammatory skin disorders. *J. Med. Chem*. **2018**, *61*, 4436–4455.

[37] Ayoup, M. S.; Wahby, Y.; Abdel-Hamid, H.; Ramadan, E. S.; Teleb, M.; Abu-Serie, M. M.; Noby, A. Design, synthesis and biological evaluation of novel α-acyloxy carboxamides *via* Passerini reaction as caspase 3/7 activators. *Eur. J. Med. Chem*. **2019**, *168*, 340–356.

[38] Mostoufi, A.; Baghgoli, R.; Fereidoonnezhad, M. Synthesis, cytotoxicity, apoptosis and molecular docking studies of novel phenylbutyrate derivatives as potential anticancer agents. *Comput. Biol. Chem*. 2019, 80, 128–137.

[39] Zhou, S.; Liao, H.; He, C.; Dou, Y.; Jiang, M.; Ren, L.; Zhao, Y.; Gong, P. Design, synthesis and structureeactivity relationships of novel 4-phenoxyquinoline derivatives containing pyridazinone moiety as potential antitumor agents. *Eur. J. Med. Chem*. 2014, 83, 581–593.

[40] Estévez, V.; Villacampa, M.; Menéndez, J. C. Recent advances in the synthesis of pyrroles by multicomponent reactions. *Chem. Soc. Rev*. **2014**, *43*, 4633–4657.

[41] Kim, K. S.; Zhang, L.; Schmidt, R.; Cai, Z. -W.; Wei, D.; Williams, D. K.; Lombardo, L. J.; Trainor, G. L.; Xie, D.; Zhang, Y.; An, Y.; Sack, J. S.; Tokarski, J. S.; Darienzo, C.; Kamath, A.; Marathe, P.; Zhang, Y.; Lippy, J.; Jeyaseelan Sr, R.; Wautlet, B.; Henley, B.; Gullo-Brown, J.; Manne, V.; Hunt, J. T.; Fargnoli, J.; Borzilleri, R. M. Discovery of pyrrolopyridine-pyridone based inhibitors of Met kinase: synthesis, X-ray crystallographic analysis, and biological activities. *J. Med. Chem*. **2008**, *51*, 5330–5341.

[42] Peach, M. L.; Tan, N.; Choyke, S. J.; Giubellino, A.; Athauda, G.; Burke, Jr., T. R.; Nicklaus, M. C.; Bottaro, D. P. Directed discovery of agents targeting the Met tyrosine kinase domain by virtual screening. *J. Med. Chem*. **2009**, *52*, 943–951.

Entry for the Table of Contents

Design, Synthesis and Biological Evaluation of Novel α-Acyloxycarboxamide-Based Derivatives as c-Met Inhibitors

Yu-juan Feng,[‡,a,b] Yu-Lin Ren,*[,‡,a,b] Li-Ming Zhao,*[,a,b] Guo-Qiang Xue,[a,b] Wen-Hao Yu,[a,b] Jia-Qi Yang,[a,b] and Jun-Wei Liu [a,b]

Chin. J. Chem. **2021**, *39*, XXX—XXX. **DOI: 10.1002/cjoc.202100XXX**